

Modeling of network degradation in mixed step-chain growth polymerizations

Sirish K. Reddy^a, Kristi S. Anseth^{a,b}, Christopher N. Bowman^{a,c,*}

^aDepartment of Chemical and Biological Engineering, University of Colorado, Boulder, CO 80309-0424, USA

^bHoward Hughes Medical Institute, University of Colorado, Boulder, CO 80309, USA

^cDepartment of Restorative Dentistry, University of Colorado Health Sciences Center, Denver, CO 80045-0508, USA

Available online 19 March 2005

Abstract

The ability to form degradable hydrogels having controlled network structure is important for applications related to both drug delivery and tissue engineering. Although significant advances have occurred, these applications cannot reach full potential without the availability of materials with tunable degradation behavior. Here, we present novel thiol–acrylate degradable networks, which provide a simple method for forming degradable networks having specific degradation profiles. Degradable thiol–acrylate networks are formed from copolymerizing a thiol monomer with PLA-*b*-PEG-*b*-PLA based diacrylate macromers. A theoretical model has been developed to describe the kinetic chain length distribution, the bulk degradation behavior, and the reverse gelation point of these thiol–acrylate hydrogels. Varying the thiol functionality, as well as the relative stoichiometries of the thiol and acrylate functional groups, provides a facile means to control the kinetic chain length distribution and the concomitant degradation behavior of these systems. The extent of percentage mass loss of the network at the reverse gelation point is controlled from as low as 30% to as high as 95%, thereby giving the unique ability to dictate the material properties of the hydrogel before the network becomes completely soluble.

© 2005 Elsevier Ltd. All rights reserved.

Keywords: Hydrogel; Acrylate; Gelation

1. Introduction

Degradable materials have gained significant importance in medical, environmental, and other applications. The widespread interest in these materials is primarily due to their potential in forming resorbable scaffolds for tissue engineering applications and site-specific drug delivery vehicles without the necessity for retrieval. One class of degradable materials, hydrogels, which are hydrophilic, crosslinked polymers, are currently receiving interest for use in a wide variety of medical applications ranging from contact lenses to drug delivery devices [1,2]. Hydrogels swell to a great extent in water due to their hydrophilic character but do not dissolve due to their crosslinked nature, yielding characteristics similar to soft tissues. Degradable hydrogels offer many of the same advantages of typical

hydrogels but also contain chemical units in the network structure that cleave either hydrolytically or enzymatically [3–5]. This degradation mechanism facilitates their use as scaffolds for controlled tissue regeneration as well as matrices for drug administration, particularly for hydrophilic compounds such as proteins and oligonucleotides [6–11].

The ability to form hydrogels in vivo through photopolymerization greatly benefits medical applications as complex structures are formed that adhere well to the surrounding tissues. Photopolymerization rapidly converts liquid monomers into crosslinked structures, utilizing visible or UV light. Photopolymerization affords several advantages over conventional polymerization techniques, including rapid polymerization rates, spatial and temporal control over polymerization, and minimal heat production.

Sawhney et al. [3] originally addressed the synthesis of water soluble macromers that are photopolymerizable and react to form biodegradable polymeric hydrogels. These macromers, which are triblock poly(lactic acid)–poly(ethylene glycol)–poly(lactic acid) copolymers (PLA-*b*-PEG-*b*-PLA) with acrylate end groups, are readily polymerized

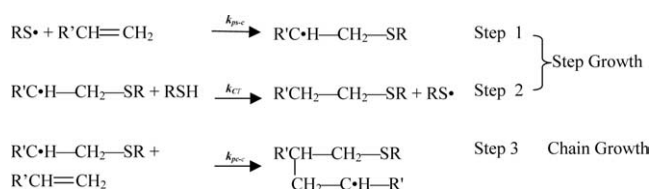
* Corresponding author. Tel.: +1 303 492 3247; fax: +1 303 492 4341.
E-mail address: christopher.bowman@colorado.edu (C.N. Bowman).

through the acrylate end groups to form hydrogels that degrade through hydrolytic cleavage of the PLA units within the gel crosslinks. Extensive studies have been conducted on controlling the network formation and the concomitant degradation of the crosslinked hydrogels formed from multifunctional monomers [6,8,12–15]. A comprehensive understanding of the network degradation and mass loss profiles of these bulk eroding hydrogels was further provided by theoretical modeling approaches [15–17]. These works on degradable hydrogels indicate that there is a strong impact of the macromer functionality and chemistry as well as polymerization conditions on the hydrogel degradation [8,16,18]. However, while control over the number of crosslinks per kinetic chain, which significantly impacts the degradation kinetics [16], is quite limited with typical acrylate polymerizations, controlling the degradation kinetics through changes in the degradable chemistry involves design and synthesis of new macromers. Further, polymerizations of macromers in varying concentrations, as a means to vary the number of crosslinks per kinetic chain, significantly affects the initial mechanical and swelling behavior along with changing the degradation behavior. Recently, Hubbell and coworkers investigated networks formed from Michael addition type reactions between thiol and acrylate monomers [19,20]. These networks are formed through step-growth polymerization and provide enhanced control over the network structure. Michael addition between thiol and acrylate monomers is mediated by slightly basic environment. However, it is not possible to have spatial or temporal control on the materials formed from this route.

Here, we are interested in photopolymerizing acrylated PLA-*b*-PEG-*b*-PLA macromers with multifunctional thiol comonomers. Copolymerization of multifunctional, acrylated PLA-*b*-PEG-*b*-PLA macromers with thiol comonomers leads to the formation of crosslinked, degradable thiol-acrylate networks. This copolymerization reaction occurs through a mixed mode growth mechanism that is radical mediated but combines features of both step and chain growth polymerizations. The resulting network's properties are easily controlled with changes in either the thiol functionality or its relative stoichiometric concentration.

Previously, a very limited number of investigations have been conducted on thiol-acrylate photopolymerizations [21–25]. Thiol-acrylate polymerizations are radical reactions that proceed via a unique mixed step-chain growth mechanism. The unique thiol-acrylate propagation mechanism is outlined below [26,27]. The thiyl radical propagates through the vinyl functional group to form a carbon based radical (step 1). This carbon-based radical either chain transfers to a thiol to regenerate a thiyl radical (step 2) or homopolymerizes with vinyl moieties (step 3). In the case of vinyl moieties that do not readily homopolymerize, as in pure thiol-ene reactions, the basic reaction mechanism is sequential propagation-chain transfer mechanism that leads to step growth polymerization. For most

thiol-ene systems, the step growth mechanism dominates over the chain growth homopolymerization of the ene monomers [23]; however, in thiol-acrylate systems, where the acrylic vinyl monomer undergoes significant homopolymerization, a competition exists between step growth and chain growth mechanisms. Thus, in thiol-acrylate systems the polymerization reaction is a combination of both chain growth and step growth polymerization mechanisms. The balance of these two mechanisms controls the network structure and, ultimately, the degradation behavior.



Previous researchers have translated this combination of mechanisms into specie balances and kinetic equations for these systems as presented in Eq. (1) [23,27]. In arriving at Eq. (1), a pseudo steady state assumption was used along with specie balance on the thiyl radical concentration ($k_{CT}C\cdot[\text{SH}] = k_{ps-c}S\cdot[\text{C}=\text{C}]$). The specie balance equation on the thiyl radical concentration accounts for the generation (step 2) or consumption (step 1) of thiyl radicals through chain transfer and propagation mechanisms. These investigations further found that the ratio of k_{pc-c}/k_{CT} in several thiol-acrylate systems was approximately 1.5.

$$\begin{aligned}
 \frac{d[\text{C}=\text{C}]}{d[\text{SH}]} &= \frac{k_{ps-c}S\cdot[\text{C}=\text{C}] + k_{pc-c}C\cdot[\text{C}=\text{C}]}{k_{CT}C\cdot[\text{SH}]} \\
 &= 1 + \frac{k_{pc-c}[\text{C}=\text{C}]}{k_{CT}[\text{SH}]} \quad (1)
 \end{aligned}$$

Here, $[\text{C}=\text{C}]$ and $[\text{SH}]$ represent the acrylate and thiol concentrations, respectively. k_{pc-c} gives the propagation constant of the acrylate, and the chain transfer constant of acrylic radical to thiol monomer is given by k_{CT} .

Thiol-vinyl polymerizations, both the thiol-ene and the thiol-acrylate polymerizations, exhibit all the advantages of typical acrylate photopolymerizations including spatial and temporal control over polymerization and excellent material properties. Further, these reactions have several advantages over acrylate polymerizations including rapid curing in the presence of little or no initiator [28–31], reduced sensitivity to oxygen inhibition [28,29,32,33], lower volume shrinkage [34], and delayed gelation.

In this study we describe theoretically the bulk degradation profiles of degradable thiol-acrylate systems using modeling approaches where all the parameters are related to physically relevant aspects of the system. As the degradation behavior is severely impacted by the number of crosslinks per kinetic chain [16], we first develop a route to estimate the kinetic chain length distribution in these systems. The bulk degradation model based on probability and mean field kinetics is then utilized to predict the

degradation phenomena of the model thiol–acrylate degradable networks. This modeling approach is extendable to other crosslinked, bulk degradable hydrogel networks that are formed through mixed step-chain polymerizations.

2. Results and discussion

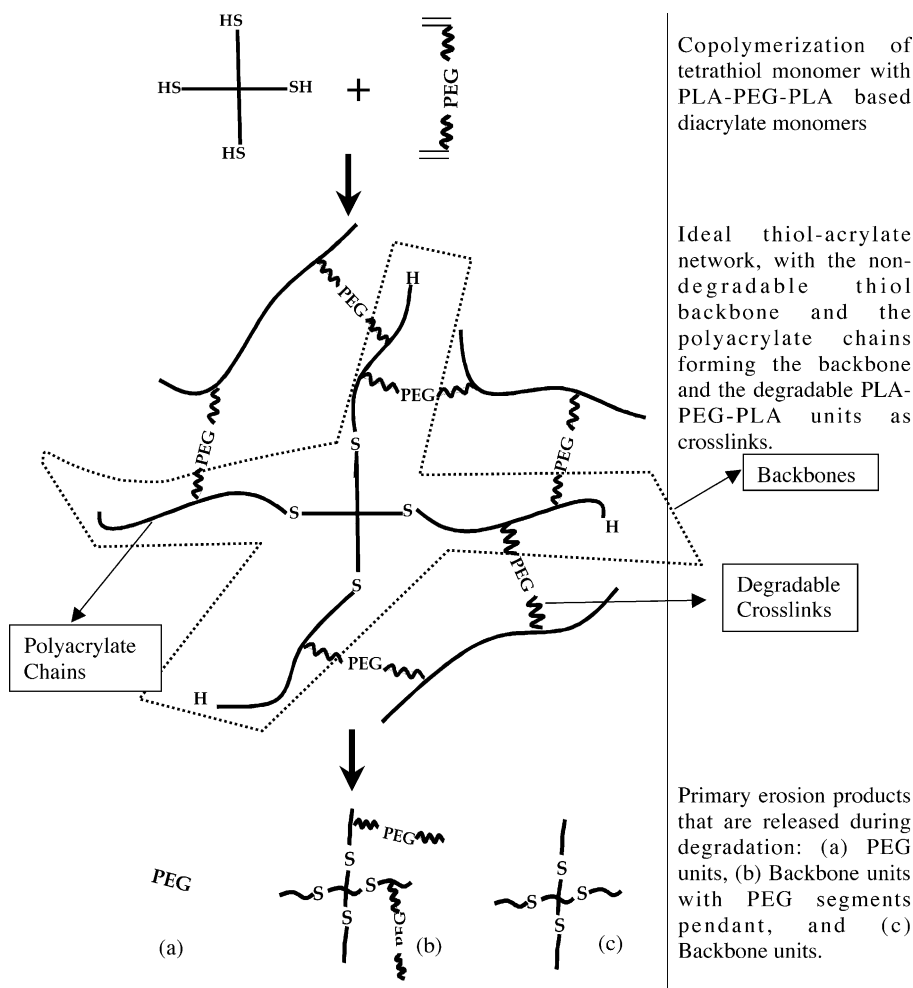
A three-dimensional network is formed when thiol and multifunctional degradable acrylate monomers are copolymerized. The resultant network is a degradable system having non-degradable backbones, consisting of the thiol monomer and short polyacrylate chains emanating from it, and the degradable PLA-*b*-PEG-*b*-PLA crosslinks connecting these backbones to the network (see Scheme 1 for an illustration). The microscopic cleavage of the lactide units leads to the bulk degradation of the formed hydrogels, and upon complete hydrolysis, the degradation products consist of the PEG units, lactic acid units, and the non-degradable backbones (Scheme 1). In this work, cyclization of acrylates is neglected to simplify the model calculations.


Previous degradation modeling of crosslinked hydrogels has revealed a strong impact of the number of crosslinks per kinetic chain on the polymer degradation and mass loss profiles [16]. Here, the nature of the thiol–acrylate polymerization provides a facile means for controlling the kinetic chain length over a much greater range than possible otherwise. Although a complete examination of the network evolution of thiol–acrylate systems is beyond the scope of this study, the kinetic chain length evolution, which impacts the degradation kinetics of the formed polymer, is addressed here. A bulk degradation model based on elementary probability is then used to show the impact of kinetic chain lengths on degradation profiles.

2.1. Structural evolution of thiol–acrylate systems

2.1.1. Kinetic chain length of polyacrylate chains attached to a thiol functionality

In thiol–acrylate systems the relative magnitudes of propagation and chain transfer rates have a significant impact on the polymer network structure and the resulting



Scheme 1. Illustration of the network formation of thiol–acrylate hydrogels and their subsequent degradation. The degradable polylactide units are represented by .

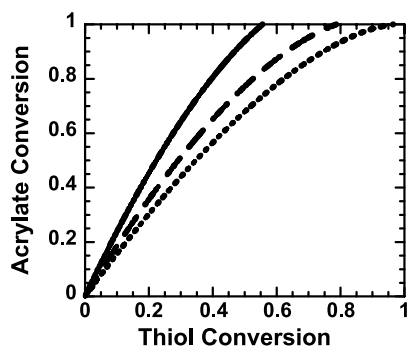


Fig. 1. Model predictions for the relative consumption of thiol and acrylate functional groups in thiol–acrylate polymerizations with various stoichiometric ratios of thiol and acrylate groups. 50:50 thiol/acrylate (—), 30:70 thiol/acrylate (---), 10:90 thiol/acrylate (•••).

material properties. While homopolymerization leads to an increase in chain length, the chain transfer step effectively terminates the growing kinetic chain. Fig. 1 plots the predicted double bond conversion as a function of thiol conversion for various initial stoichiometric ratios of thiol and acrylate functional groups. It is evident from the plot that the final thiol conversion is highly dependent on the initial stoichiometric ratio, and it decreases with increasing fraction of thiol monomer in the initial mixture. Further, the average number of acrylic monomers attached per thiol functional group, given by the slope of the curve, changes both with the initial stoichiometric ratio and with the extent of conversion, thereby giving rise to a distribution of kinetic chain lengths and a highly complex network structure.

In the polymerization of a monothiol–acrylate system, where the thiol moiety has only one reacting functional group per monomer, the average kinetic chain length is simply given by the average number of acrylate units that a radical consumes prior to chain transfer to thiol monomer. Therefore, the average kinetic chain length in the monothiol–acrylate system is given by the ratio of consumption of acrylate monomers to thiol monomer consumption. As Eq. (1) gives the consumption of acrylate monomers per thiol monomer consumption ($d[C=C]/d[SH]$), the expression $1 + k_{pc-c}[C=C]/k_{CT}[SH]$ equals the kinetic chain length in this system. While at any given conversion, the average kinetic chain length (KCL) is given by Eq. (1), it is also possible and important to determine their distribution. The acrylic radical homopolymerizes with a probability (p_h) of $k_{pc-c}[C=C]/[k_{CT}[SH] + k_{pc-c}[C=C]]$, while chain transferring with a probability $(1-p_h)$ of $k_{CT}[SH]/[k_{CT}[SH] + k_{pc-c}[C=C]]$. The probability that a thiol functional group is attached to n acrylic units is given by the probability that the first acrylic radical, which is formed from the propagation of a thyl radical through the double bond, is attached to $n-1$ acrylic units. The probability that the acrylic radical propagates along $n-1$ acrylic monomers before chain transferring is given by Eq. (2). This equation also gives the number fraction KCL distribution at a given extent of conversion.

$$p(n) = p_h^{(n-1)}(1 - p_h) \quad (2)$$

Further, as the relative ratio of functional groups varies with conversion (Fig. 1) and as the KCL distribution is a function of both the thiol and acrylic functional group concentrations, the overall distribution of kinetic chains is given by a summation of KCL distributions at each conversion. Fig. 2(a) plots the number fraction distribution of KCLs for a 10:90 stoichiometric ratio of monothiol/acrylate. As expected from Eq. (2), there is a monotonic decrease in the number fraction of chains as the KCL increases. Interestingly, as shown later, the weight fraction molecular weight distribution has a more profound impact on the degradation kinetics, and Fig. 2(b) presents the weight fraction KCL distribution of in the 10:90 monothiol/acrylate system.

In a copolymerization of multifunctional thiol monomers ($f_1 > 1$) with acrylate monomers, each thiol functional group on a monomer may be initiated at a different point in the polymerization. Hence, the distribution of the kinetic chains per backbone for this case would be given by statistical averaging of the length of polyacrylate chains on each arm of the thiol monomer. Here, the distribution of the

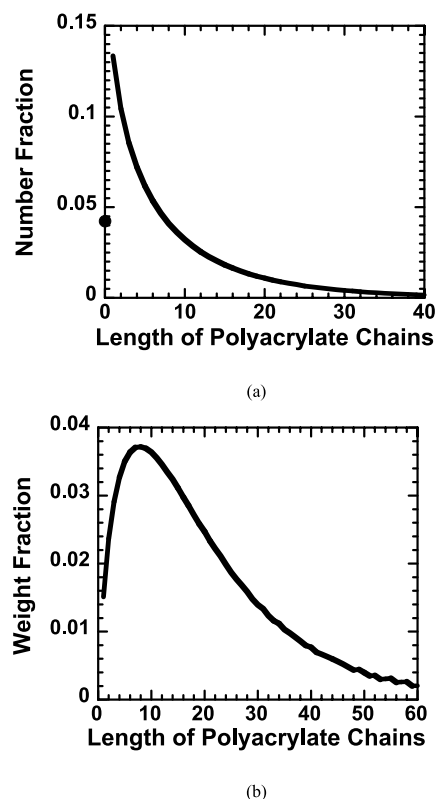


Fig. 2. Theoretical distributions of (a) number fraction kinetic chain lengths and (b) weight fraction kinetic chain lengths for a 10:90 stoichiometric ratio of mono-thiol: acrylate system. The x-axis of the plot represents the number of acrylic units attached to a thiol group (length of polyacrylate chains), while the y-axis represents the corresponding fraction of thiol groups with that acrylate length attached. The number fraction of thiol monomers that are unreacted and hence attached to zero acrylate units is represented by •.

number of acrylate monomers attached per thiol functional group is represented by the multinomial expression: $Y = a_0x^{n_0} + a_1x^{n_1} + \dots + a_{N_{MAX}-1}x^{n_{MAX-1}} + a_{N_{MAX}}x^{n_{MAX}}$, wherein a_i represent the fraction of thiol groups attached to n_i acrylate units (Fig. 2). Then, the weight fraction of multifunctional thiol units that have a total of m acrylates attached to it is known to be the coefficient of x^m in the above expression raised to the power of the thiol functionality. This fraction accounts for all possible combinations of n_i acrylates on each arm of the thiol monomer. For example, we utilize the KCL distribution of a 10:90 monothiol/acrylate system (Fig. 2), and thereby determine using the multinomial theorem the resulting weight fraction KCL distribution for a 10:90 dithiol/acrylate system (Fig. 3).

2.1.2. Influence of stoichiometry and thiol functionality on the chain length distribution

The stoichiometry and thiol functionality have a significant impact on the network properties of thiol–acrylate systems. The impact of thiol concentration and functionality on the network properties is addressed here both schematically and through model predictions.

2.1.3. Impact of stoichiometry

It is evident from Fig. 1 that the initial stoichiometric ratio of thiol/acrylate functional groups impacts the relative consumption of the functional groups and may be utilized to change the average number of acrylates added per thiol. This aspect of control is shown in Scheme 2. It can be observed from the scheme that the relative homopolymerization rate is easily controlled by changing the stoichiometry of the mixture, thereby presenting an extremely simple method for tuning the KCLs and the number of crosslinks per kinetic chain in the resulting network. If the crosslinks are degradable, then changing the number of crosslinks per backbone dictates the degradation profile of the resulting networks.

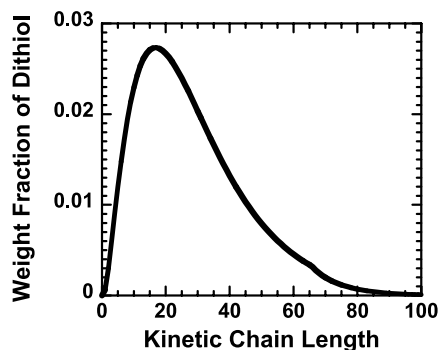
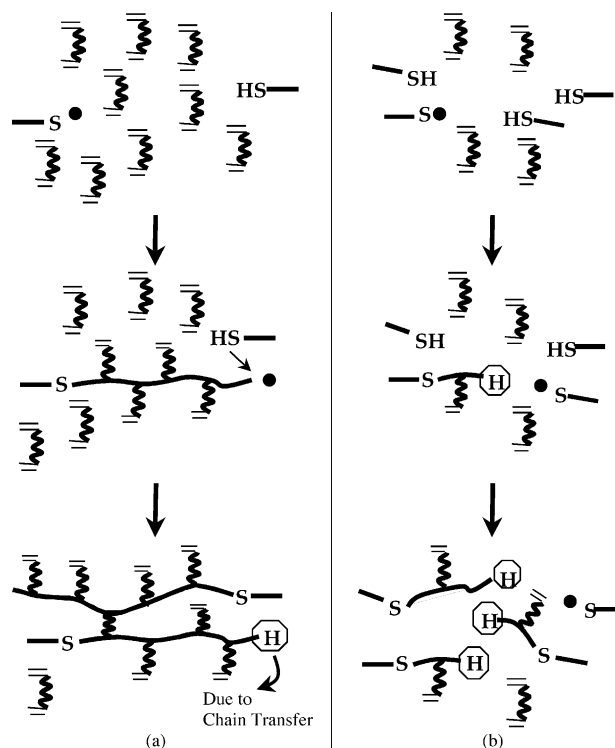


Fig. 3. Theoretical distribution of weight fraction of kinetic chain lengths for a difunctional thiol and acrylate system, with a 10:90 stoichiometric ratio. The x -axis of the plot represents the kinetic chain lengths of the backbones. The kinetic chain length of the backbone is given by statistical averaging of the length of polyacrylate chains on each of the arms of the thiol monomer. The y -axis represents the corresponding weight fraction of thiol groups with that acrylate length attached.



Scheme 2. Impact of thiol concentrations on number of acrylate groups attached per thiol group. Lower thiol concentrations lead to chains having longer chain lengths (a) while higher thiol concentrations leads to higher chain transfer rates and thus form chains having a higher number of acrylates attached per thiol group. Non-degradable backbones are represented by \sim and the degradable crosslinks by \sim .

The impact of the initial stoichiometric ratio on the weight fraction KCL distribution is shown in Fig. 4. The plot shows the predicted distribution of KCLs for two different thiol–acrylate mixtures, 30:70 and 10:90 stoichiometric ratios of dithiol/acrylate. As expected from Scheme 2, the plot portrays a decrease in KCLs with an increase in the thiol concentrations.

2.1.4. Impact of thiol functionality

In a thiol–acrylate system the network evolution is not

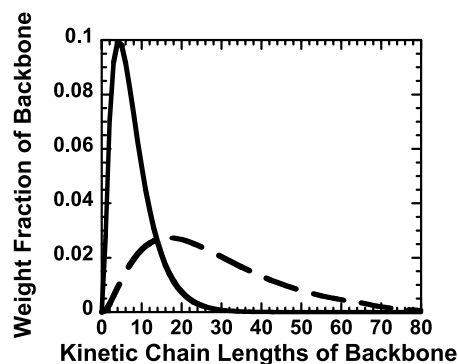
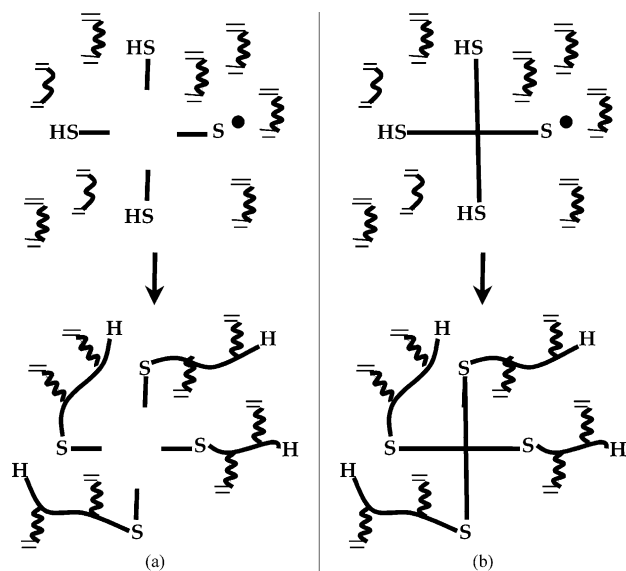


Fig. 4. Plot displaying the theoretical distributions of kinetic chain lengths for 30:70 (—) and 10:90 (---) stoichiometric ratio of difunctional thiol:acrylate mixtures.



Scheme 3. Influence of thiol functionality on number of crosslinks attached per non-degradable backbone. Copolymerizing a diacrylate monomer having a degradable spacer with monothiol (a) leads to chains having fewer number of degradable units while compared to networks formed upon curing multifunctional (here tetrafunctional) thiol monomers (b). Non-degradable backbones are represented by and the degradable crosslinks by .

solely a function of functional group stoichiometry, but it is also impacted by the thiol functionality. This aspect of network control is shown in Scheme 3. This scheme demonstrates that the KCL of the backbone is controlled by changing the thiol monomer functionality, even while maintaining the relative functional group stoichiometry. Increasing the thiol functionality increases the number of polyacrylate chains that are attached to the thiol monomer and hence the KCL of the network backbone.

Fig. 5 compares the predicted chain length distribution for networks formed from the copolymerization of an acrylate monomer with a difunctional thiol and a tetrafunctional thiol. The relative stoichiometry of thiol to acrylate functional groups in both these systems is kept at 10:90. As

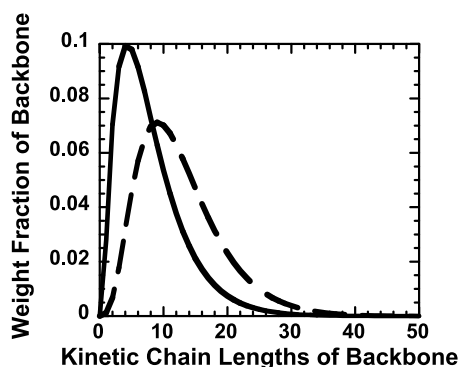


Fig. 5. Plot comparing the theoretical distributions of kinetic chain lengths of a 30:70 thiol/acrylate system, formed from copolymerization of the acrylate monomer with a difunctional thiol monomer (—) and a tetrafunctional thiol monomer (---).

indicated by Scheme 3, the KCL increases with increasing thiol functionality.

2.2. Development of bulk-degradation model

The bulk degradation modeling approach used here is based on a statistical mean-field approach and elementary probability theories. This work utilizes principles similar to those that were developed previously to predict the bulk-degradation of crosslinked hydrogels formed from pure chain growth polymerizations [16,18]. However, this model improves upon the estimation of the reverse gelation point by utilizing the recursive nature of polymer networks. Further, knowledge of the KCL distributions is used to enhance the model predictions.

In this model the lactic acid oligomers within each copolymer segment are considered as a single degradable PLA unit. Hence, the PEG unit in the PLA-*b*-PEG-*b*-PLA copolymer is flanked on either side by one degradable site. Because of the high degree of swelling exhibited by the PLA-*b*-PEG-*b*-PLA gels when placed in an aqueous environment, the hydrolytical cleavage of each PLA unit is assumed to occur homogeneously throughout the network, independent of position and time. Further, due to the high water content of the hydrogels, the hydrolytic cleavage of the PLA units was assumed to occur through a pseudo first order reaction. Here, the concentration of the degradable polylactide unit is represented by P and its first order degradation constant is indicated by k' . $[PLA]_0$ denotes the initial concentration of poly lactide units. In probability terms the probability (P) of a random PLA unit being hydrolyzed is given by the fraction of all PLA units that have been hydrolyzed.

$$\frac{d[PLA]}{dt} = -k'[PLA] \Rightarrow [PLA] = [PLA]_0 e^{-k't} \quad (3)$$

$$P = 1 - \frac{[PLA]}{[PLA]_0} = 1 - e^{-k't}$$

Mass loss in the model is estimated by calculating the probability that a certain species is released from the network, and this mass loss is ultimately described as a function of the extent of PLA degradation. Combining Eq. (3) with the knowledge of the network architecture relates the PLA unit degradation to the network erosion profile. Neglecting the individual lactic acid units, the three primary soluble degradation products are (i) PEG chains, (ii) thiol-acrylate backbones, and (iii) the thiol-acrylate backbones attached to the uncleaved PLA-*b*-PEG-*b*-PLA segments. These species are considered eroded or released when all the bonds connecting them to the network are broken. As can be seen in Scheme 1, erosion and subsequent release of these species occurs due to hydrolytical cleavage of the PLA units and release depends on the connectivity of each of these species to the network. As shown from previous modeling work on similar systems, it can be assumed that the diffusion

of degradable species out of the swollen network occurs much more rapidly than the degradation [17]. Hence, it can be safely assumed that once a specie is completely cleaved from the network backbone, the product appears as mass loss.

As the mass loss in PLA-*b*-PEG-*b*-PLA based hydrogels is associated with the cleavage of PLA units, it is very important to incorporate structural aspects of the hydrogel network into the degradation model. As outlined by Metters et al. [16,17], in a degrading hydrogel the PLA-*b*-PEG-*b*-PLA segment, which serves as a crosslinker, exists in one of three states: (i) an intact segment, in which neither of the PLA units are cleaved; (ii) only one of the PLA units is cleaved, in which case the segment exists as a pendant chain; and (iii) both the PLA units are cleaved, thereby releasing the segment from the network. The fraction of PLA-*b*-PEG-*b*-PLA segments in any of these three states is calculated through elementary probabilities and expressed as a function of the extent of degradation of PLA units (P).

(i) Fraction of PLA-*b*-PEG-*b*-PLA segments which are intact, i.e. neither of the PLA units are degraded.

$$y_1 = (1 - P)^2 \quad (4)$$

(ii) Fraction of PLA-*b*-PEG-*b*-PLA segments that are dangling from the network backbone, i.e. only one of the PLA units is degraded.

$$y_2 = 2P(1 - P) \quad (5)$$

(iii) Fraction of PLA-*b*-PEG-*b*-PLA segments that are released, i.e. both the PLA units are cleaved.

$$y_3 = P^2 \quad (6)$$

As stated earlier, any specie in the network is released only after all bonds attaching it to the network are cleaved. Hence, for the release of a portion of the thiol-acrylate network backbone, all the crosslinking units connecting it to the network must be degraded. Mathematically speaking, the fraction of the backbone units (F_{BB}) released from the network is given by the probability that all the crosslinks attached to backbone exist in either state (ii) or state (iii), i.e. none of the crosslinks is completely intact. For example, a chain with N crosslinks has a fractional probability of being released, $F_{BB}(N)$:

$$F_{BB}(N) = (y_2 + y_3)^N = (2P(1 - P) + P^2)^N \quad (7)$$

Hence, to calculate the overall backbone fraction released, we must account for chains of all lengths:

$$\begin{aligned} F_{BB} &= \sum W_{BB,i} F_{BB}(N_i) = \sum W_{BB,i} (y_2 + y_3)^{N_i} \\ &= \sum W_{BB,i} (2P(1 - P) + P^2)^{N_i} \end{aligned} \quad (8)$$

where N_i indicates the KCL of the backbone. $W_{BB,i}$ represents the weight fraction of backbones that have N_i crosslinks and is given by

$$W_{BB,i} = \frac{A_i N_i}{\sum A_i N_i} \quad (9)$$

Here, A_i gives the fraction of backbone units that have N_i crosslinks attached to them. The overall expression for F_{BB} is given by

$$\begin{aligned} F_{BB} &= \sum \frac{A_i N_i}{\sum A_i N_i} (y_2 + y_3)^{N_i} \\ &= \sum \frac{A_i N_i}{\sum A_i N_i} (2P(1 - P) + P^2)^{N_i} \end{aligned} \quad (10)$$

As the distribution of N_i versus A_i is known (Fig. 2), Eq. (10) is easily solved to determine the fraction of eroded backbone units (F_{BB}) as a function of time or PLA degradation extent.

Once F_{BB} is known, the fraction of PLA-*b*-PEG-*b*-PLA units released (F_{PEG}) from the network is calculated using the same approach as Metters et al. [16] As stated earlier, PLA-*b*-PEG-*b*-PLA units exist in three states. Individual PEG chains are released when the PLA-*b*-PEG-*b*-PLA segments exist in state three with both PLA units hydrolytically cleaved. PLA-*b*-PEG-*b*-PLA segments that exist in state two are released only when the backbone units from which the segments are dangling are released. F_{PEG} is hence composed of two terms: (a) the fraction of PLA-*b*-PEG-*b*-PLA segments for which both PLA units are cleaved and (b) the fraction of PEG segments that are dangling from an eroded backbone segment.

$$F_{PEG} = y_3 + F_{BB} \frac{y_2}{2} = P^2 + F_{BB} P(1 - P) \quad (11)$$

Knowing the fraction of building blocks of the hydrogel that have been released, the overall mass loss calculation is relatively simple:

$$\% \text{ Mass Loss} = (W_{BB} F_{BB} + W_{PEG} F_{PEG}) \quad (12)$$

Here, F_{BB} represents the fraction of backbone units released from the network, while F_{PEG} represents the fraction of PEG units released. Similarly, the mass percents of the backbone and PEG units are represented by W_{BB} and W_{PEG} , respectively.

As the building blocks of the hydrogel degrade, a limit is achieved where the chains in the bulk degrading system no longer form an infinite molecular weight gel. At this 'reverse gelation' point, the network becomes a collection of highly branched, soluble uncrosslinked polymer chains. This feature is essentially the inverse process of gelation as observed during the formation of polymer networks. At the reverse gelation point the entire network is water soluble.

A recursive approach, similar to the method utilized by Miller and Macosko [35,36], is employed here for determining the reverse gelation point. This approach uses the recursive nature of branching processes and the elementary law of conditional probability.

Law of conditional probability: If A is an event and A' is the complementary event. Let us represent a random

variable by W , its expected value, $E(W)$ and the conditional probability of W given the event A by $E(W|A)$. Then the law of conditional probability states:

$$E(W) = E(W|A)P(A) + E(W|A')P(A') \quad (13)$$

First, we examine a simple case, where there is no crosslink distribution and every backbone unit is attached to N crosslinks. In the case of degrading hydrogels the reverse gelation point is associated with the formation of an uncrosslinked gel, due to the degradation of PLA units. Hence, we first look at the possible states of the degradable segments: (i) PLA-*b*-PEG-*b*-PLA segment cleaved on both sides, (ii) PLA-*b*-PEG-*b*-PLA cleaved on only side and hence the chain acting as a dangling unit, and (iii) PLA-*b*-PEG-*b*-PLA segment intact. The probabilities of these events are related to the extent of PLA degradation by Eqs. (4)–(6).

As we are interested in knowing the reverse gelation point, the variable of interest is the weight attached to a crosslink. So, we pick up a PLA-*b*-PEG-*b*-PLA segment at random and examine the weight attached to it, looking out from its parent molecule.

$$\begin{aligned} E(W_{\text{out}}) &= E(W_{\text{out}}|\text{Degradable segment intact}) \\ &\times P(\text{Degradable segment intact}) \\ &+ E(W_{\text{out}}|\text{Degradable segment cleaved on one side}) \\ &\times P(\text{Degradable segment cleaved on one side}) \\ &+ E(W_{\text{out}}|\text{Degradable segment cleaved on both sides}) \\ &\times P(\text{Degradable segment cleaved on both sides}) \end{aligned} \quad (14)$$

In the event that the segment is intact, the weight looking out from the PLA-*b*-PEG-*b*-PLA segment would equal the weight looking into another backbone chain. However, in the other two cases where the segment is cleaved on either side, the weight looking out from the segment would not equal the weight looking into another backbone. Specifically, in the case of a segment cleaved on only one side, the weight looking out from the segment is zero, while the weight looking from a segment which is dangling from the parent molecule equals the weight of a PEG unit.

$$E(W_{\text{out}}) = E(W_{\text{in}})(1 - P)^2 + W_{\text{PEG}} \frac{2P(1 - P)}{2} + 0(P^2) \quad (15)$$

$E(W_{\text{in}})$, the expected weight of a segment looking into another backbone, will be the molecular weight of the nondegradable backbone unit, M_{BB} , plus the sum of the expected weights on each of the remaining $N - 1$ arms with $E(W_{\text{out}})$ for each arm.

$$E(W_{\text{in}}) = M_{\text{BB}} + (N - 1)E(W_{\text{out}}) \quad (16)$$

The recursive nature of this equation leads us back to the starting situation.

Solving Eqs. (15) and (16) yields

$$E(W_{\text{out}}) = \frac{M_{\text{BB}}(1 - P)^2 + W_{\text{PEG}}P(1 - P)}{1 - (1 - P)^2(N - 1)} \quad (17)$$

It is observed from the above equation that when $(1 - P)^2(N - 1) > 1$, the solution to Eq. (17) does not exist and the system remains gelled. However, as the degradation of PLA units (P) increases, $(1 - P)^2(N - 1) < 1$ and the network ceases to exist as a crosslinked gel. This extent of degradation (P_{rg}) at which this transition occurs is given by:

$$P_{\text{rg}} = 1 - \frac{1}{\sqrt{N - 1}} \quad (18)$$

So, the reverse gelation point, or the extent of degradation at which the network becomes completely soluble, is given by Eq. (18) for a hydrogel which has N crosslinks. Now we will examine our case, wherein we have a distribution of crosslinks. Eq. (15), which describes the relationship between the weight looking out from one backbone to another backbone unit does not change; however, Eq. (16) must be modified to account for the distribution of the number crosslinks.

$$\begin{aligned} E(W_{\text{in}}) &= \sum W_{\text{BB},i} \{M_{\text{BB}} + (N_i - 1)E(W_{\text{out}})\} \\ &= \sum W_{\text{BB},i} M_{\text{BB}} + \sum \frac{A_i N_i (N_i - 1)}{\sum A_i N_i} E(W_{\text{out}}) \\ &= M_{\text{BB}} \sum W_{\text{BB},i} + \left[\frac{\sum A_i N_i}{\sum A_i N_i} - 1 \right] E(W_{\text{out}}) \\ &= M_{\text{BB}} + (N_{\text{Wt,Avg}} - 1)E(W_{\text{out}}) \end{aligned} \quad (19)$$

where

$$N_{\text{Wt,Avg}} = \frac{\sum A_i N_i}{\sum A_i N_i}$$

Eq. (19), which takes into account the distribution of crosslinks, is similar to Eq. (16), except that the number of crosslinks for a system having a distribution of crosslinks is replaced by the weight average number of crosslinks. Using Eqs. (19) and (15), we obtain

$$E(W_{\text{out}}) = \frac{M_{\text{BB}}(1 - P)^2 + W_{\text{PEG}}P(1 - P)}{1 - (1 - P)^2(N_{\text{Wt,Avg}} - 1)} \quad (20)$$

and using the arguments used previously, the reverse gelation point is given by

$$P_{\text{rg}} = 1 - \frac{1}{\sqrt{N_{\text{Wt,Avg}} - 1}} \quad (21)$$

Clearly, the reverse gelation point is very sensitive to the weight average number of crosslinks per kinetic chain and hence provides an easy route to control the amount of degradation at which the network becomes completely soluble.

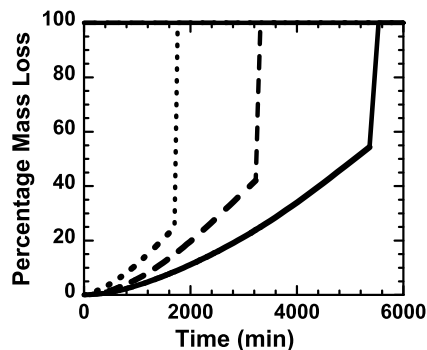


Fig. 6. Predicted percentage mass loss versus time for difunctional thiol-acrylate mixtures with 50:50 (•••), 30:70 (---), and 10:90 (—) stoichiometric ratios of dithiol/acrylate mixtures. Model parameters: $W_{BB} = W_{PEG} = 50$ wt% and $k' = 0.0003 \text{ min}^{-1}$.

2.2.1. Evaluation of the model

The number of crosslinks in the network backbone is readily changed by manipulating either the thiol concentration or functionality. Model predictions indicate that both the crosslinking density and the reverse gelation point in these networks are controlled by the thiol functionality and concentration. Fig. 6 shows the effect of thiol concentration on the mass loss predictions and compares the degradation profiles of thiol-acrylate systems prepared from 50:50 thiol/acrylate, 30:70 thiol/acrylate, and 10:90 thiol/acrylate mixtures. Three degradation regions and behaviors are readily observed from the figure. The PEG units, which are attached to the network by only two PLA units are the first chains to be released from the network. As the release of backbone chains requires the cleavage of at least one PLA unit in each of the crosslinks, the network mass loss in the initial stages is primarily PEG units. Hence, the initial mass loss profiles are nearly identical for all the systems as are the initial mechanics and swelling. As more crosslinks continue to degrade, a greater fraction of the backbone chains, along with their dangling PLA-*b*-PEG-*b*-PLA segments are released from the network. This result, however, is a strong function of the number of crosslinks per kinetic chain. As the number of crosslinks per kinetic chain decreases with increasing thiol concentration (Fig. 4), the mass loss in the second stage is accelerated for the systems formed with higher concentrations of thiol. In the final stage the degradation is characterized by reverse gelation. As the reverse gelation point depends on the number of crosslinks per backbone (Eq. (21)), the onset of this stage is dictated by the KCL of the system and hence occurs early for the system having the highest thiol concentration.

A similar effect of thiol functionality on the degradation profiles is evident from Fig. 7. This plot compares the degradation profiles of networks formed from a 30:70 thiol/acrylate system with thiol monomer functionalities (f_1) equal to 1, 2, and 4. As the KCL and the number of crosslinks per kinetic chain decrease with decreasing thiol functionality, the mass loss is rapid and the reverse gelation point occurs earlier.

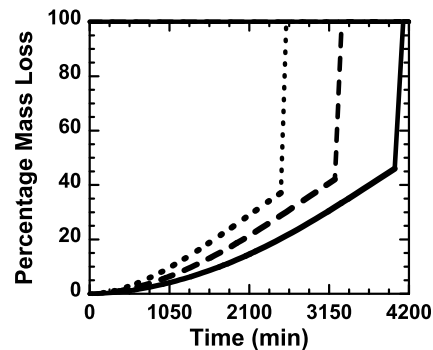


Fig. 7. Predicted percentage mass loss versus time for 30:70 thiol-acrylate mixtures using thiol monomers with functionalities of 1 (•••), 2 (---), and 4 (—). Model parameters: $W_{BB} = W_{PEG} = 50$ wt% and $k' = 0.0003 \text{ min}^{-1}$.

To demonstrate the impact of KCLs on the network degradation behavior of the crosslinked hydrogels, we compared the degradation profiles of a model thiol-acrylate system, 30:70 dithiol/acrylate system, with that of a pure acrylate system (Fig. 8). For predicting the degradation profiles of these systems, the KCL distribution and weight average KCL ($N_{Wt, Avg} = 7.94$) was calculated for the thiol-acrylate system, and a chain length of 1000 was assumed for the acrylate system. The early occurrence of reverse gelation in the thiol-acrylate systems as compared with the pure acrylate systems is expected due to the decreased KCLs in these novel systems (Eq. (21)). The rapid mass loss in these systems is also anticipated due to the lower number of crosslinks per kinetic chain in the thiol-acrylate systems. This aspect of rapid mass loss in thiol-acrylate systems is examined more closely in Fig. 9, which follows the mass loss profiles as a function of extent of PLA degradation (P) for all the primary degradation products of the networks formed from both the thiol-acrylate system and the pure acrylate system: (a) PEG segments that are cleaved on either end and hence released as free PEG units, (b) backbone units that release upon cleavage of all crosslinks, and (c) PEG segments that are released dangling to the eroded backbone units. Further, to delineate the effects of reverse gelation, this plot gives the mass loss profiles for the case of

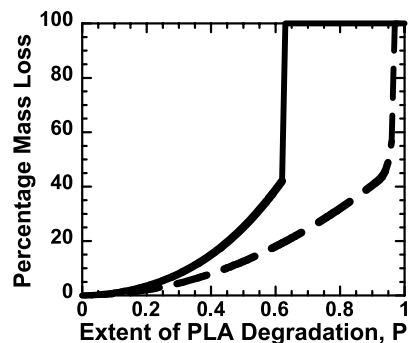


Fig. 8. Plot contrasting the degradation profiles of a thiol-acrylate system, a 30:70 dithiol/acrylate (---) network, with a network formed from pure acrylate monomers (—).

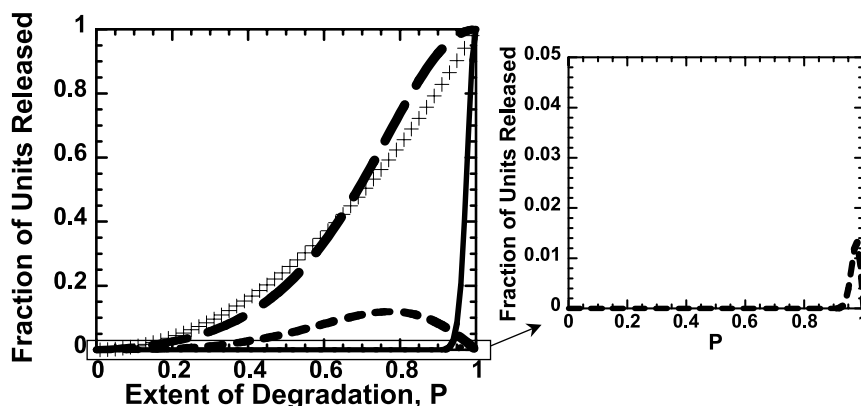


Fig. 9. Plot displaying the fraction of primary degradation products released as a function of the extent of degradation for a 30:70 thiol/acrylate system as well as for the network formed from pure acrylate monomers. The fraction of PEG units released that are cleaved on either side is represented by (+) and this fraction is the same for both the systems. The fraction of released backbones and the PEG segments that are hanging from the released backbones, in a thiol–acrylate system, are represented by (–) and (~~~~), respectively. The fraction of backbone units released from the pure acrylate system is shown by (—). The fraction of pendant PEG segments that are released due to the release of backbone chains from network formed with pure acrylate system is very small and is shown in the inset.

no reverse gelation. This plot shows two distinct features: (a) the fraction of free PEG units that are released is the same in both networks as it is given by P^2 , and (b) the fraction of released backbone units and hence associated dangling PEG units is significantly higher for the thiol–acrylate system due to its reduced KCLs. This figure clearly illustrates that the KCLs of the network not only impact the reverse gelation point but also have a significant effect on the degradation kinetics of the crosslinked hydrogels.

3. Conclusions

A bulk degradation model based on elementary probability and the mean field approach has been developed to predict the bulk degradation phenomena for model degradable hydrogel systems formed from photocuring a thiol monomer with degradable PLA-*b*-PEG-*b*-PLA based diacrylate monomers. As the degradation kinetics of hydrogels are known to be strongly dependent on the KCLs and their distribution, we have developed a framework for predicting the distribution of KCLs in these unique systems. The KCL, and hence the number of crosslinks per kinetic chain, was shown to decrease with increasing thiol concentration or decreasing thiol functionality, thus providing a facile means to control the network evolution and hence the degradation behavior. The model predictions indicate that these degradable networks, due to the changes in their KCL distributions, exhibit varied degradation kinetics with changes in the relative concentrations of thiol and acrylate monomers or by changing the thiol monomer functionality. Also, the reverse gelation point, which exhibits the strongest dependence on the number of crosslinks per kinetic chain, is well controlled through these unique step-chain growth systems.

Further, these systems, contrary to other crosslinked

hydrogel networks formed from chain growth polymerization, provide unique opportunities to estimate the number of crosslinks per kinetic chain and hence become an accurate model through which we can predict the degradation behavior of other real systems, without the need for any model fitting. The theoretical framework developed here is readily extended for predicting the degradation behavior of other crosslinked hydrogels formed from mixed step-chain growth polymerizations.

Acknowledgements

The authors would like to acknowledge their funding source for this work: NSF Industry/University Cooperative Research Center for Fundamentals and Applications of Photopolymerization and a National Science Foundation Tie Grant (EEC-0120943).

References

- [1] Peppas NA. Hydrogels in medicine and pharmacy. FL: CRC Press; 1987.
- [2] Peppas NA, Bures P, Leobandung W, Ichikawa H. Eur J Pharm Biopharm 2000;50:27–46.
- [3] Sawhney AS, Pathak CP, Hubbell JA. Macromolecules 1993;26:581–7.
- [4] Mann BK, Gobin AS, Tsai AT, Schmedlen RH, West JL. Biomaterials 2001;22:3045–51.
- [5] Luo Y, Kirker KR, Prestwich GD. J Control Release 2000;69:169–84.
- [6] Anseth KS, Metters AT, Bryant SJ, Martens PJ, Elisseeff JH, Bowman CN. J Control Release 2002;78:199–209.
- [7] Elisseeff J, Anseth K, Sims D, McIntosh W, Randolph M, Langer R. Proc Natl Acad Sci USA 1999;96:3104–7.
- [8] West JL, Hubbell JA. React Polym 1995;25:139–47.
- [9] An YJ, Hubbell JA. J Control Release 2000;64:205–15.
- [10] Chowdhury SM, Hubbell JA. J Surg Res 1996;61:58–64.

- [11] Bryant SJ, Chowdhury TT, Lee DA, Bader DL, Anseth KS. *Ann Biomed Eng* 2004;32:407–17.
- [12] Anseth KS, Quick DJ. *Macromol Rapid Commun* 2001;22:564–72.
- [13] Bryant SJ, Bender RJ, Durand KL, Anseth KS. *Biotechnol Bioeng* 2004;86:747–55.
- [14] Martens PJ, Bryant SJ, Anseth KS. *Biomacromolecules* 2003;4:283–92.
- [15] Mason MN, Metters AT, Bowman CN, Anseth KS. *Macromolecules* 2001;34:4630–5.
- [16] Metters AT, Bowman CN, Anseth KS. *J Phys Chem B* 2000;104:7043–9.
- [17] Metters AT, Anseth KS, Bowman CN. *J Phys Chem B* 2001;105:8069–76.
- [18] Martens P, Metters AT, Anseth KS, Bowman CN. *J Phys Chem B* 2001;105:5131–8.
- [19] Elbert DL, Pratt AB, Lutolf MP, Halstenberg S, Hubbell JA. *J Control Release* 2001;76:11–25.
- [20] Lutolf MP, Cerritelli S, Cavalli L, Hubbell JA. *Bioconjugate Chem* 2001;12:1051–6.
- [21] Gush DP, Ketley AD. *Mod Paint Coat* 1978;58.
- [22] Eisele G, Fouassier JD, Reeb R. *J Appl Polym Sci A-Polym Chem* 1997;35:2333.
- [23] Cramer NB, Bowman CN. *J Polym Sci Part a-Polym Chem* 2001;39:3311–9.
- [24] Reddy SK, Cramer NB, O'Brien AK, Cross T, Raj R, Bowman CN. *Macromol Symp* 2004;206:361–74.
- [25] Rydholm AE, Bowman CN, Anseth KN. *Biomaterials* 2005;26:4495–506.
- [26] Kharasch MS, Nudenberg W, Mantell GJ. *J Organ Chem* 1951;16:524.
- [27] Cramer NB, Reddy SK, O'Brien AK, Bowman CN. *Macromolecules* 2003;36:7964–9.
- [28] Cramer NB, Scott JP, Bowman CN. *Macromolecules* 2002;35:5361–5.
- [29] Reddy SK, Cramer NB, Cross T, Raj R, Bowman CN. *Chem Mater* 2003;15:4257–61.
- [30] Hoyle CE, Cole MC, Bachemin MA, Yoder B, Nguyen CK, Kuang W, et al. *RadTech Asia Techn Proc Jpn* 2000;211.
- [31] Bryant SJ, Nuttelman CR, Anseth KS. *J Biomater Sci-Polym Ed* 2000;11:439–57.
- [32] Jacobine AF, Glaser DM, Grabek PJ, Mancini D, Masterson M, Nakos ST, et al. *J Appl Polym Sci* 1992;45:471–85.
- [33] Jacobine AF. In: Fouassier JD, Rabek JF, editors. *Radiation curing in polymer science and technology III: polymerization mechanisms*. London: Elsevier Appl Science; 1993. p. 219.
- [34] Jacobine AF, Glaser DM, Nakos ST. *Photoinitiated cross-linking of norbornene resins with multifunctional thiols*. In: Hoyle CE, Kinstle JF, editors. *Radiation curing of polymeric materials*. Washington, DC: American Chemical Society; 1990. p. 161–75.
- [35] Macosko CW, Miller DR. *Macromolecules* 1976;9:206.
- [36] Miller DR, Macosko CW. *Macromolecules* 1976;9:199.